

Induction Motor Fault Feature Extraction Based on Ansoft

Xiaolei Zhang and Han Li

*School of Information and Electrical Engineering China University of Mining and
Technology*

Quan-Shan District, Xuzhou, Jiangsu Province, 221116, PR China

Email: xiaojinglingzxl@sina.com, candy_cumt@126.com

Abstract

In view of that part of motor fault state was difficult to be simulated by experiment; fault characteristic value was hard to be obtained quantitatively and so on. This paper established the finite element models of asynchronous motor in different fault conditions by Ansoft, extracted and analyzed stator current under different degree of motor broken bars, stator winding inter-turn short circuit and the air gap eccentric fault, obtained the fault characteristics with the evolution of fault degree. Finally established asynchronous motor fault experimental platform, through the comparison of the experimental data and the fault feature of the finite element models, validated the rationality of fault feature extraction method based on Ansoft.

Keywords: *Motor, The finite element analysis, Ansoft, Fault diagnosis*

1. Introduction

Induction motor has the advantages of simple structure, convenient operation and maintenance, so got very good application in all kinds of electrical drive systems and network. In case of any kind of failure will directly affect the quality of production, even a threat to the safety of staff, caused great losses, so the effective prevention and timely eliminate fault is particularly important.

Induction motor faults are mainly broken bars, stator winding inter-turn short circuit and the air gap eccentricity. The current research on motor fault can be divided into two methods, one is based on the data analysis, and the other one is based on mathematical models.

Fault diagnosis method based on data analysis contains method for graphics: for example park vector [1], holographic spectrum analysis [2-3]; neural network analysis [4-5], the information fusion technology [6-7]; stator current method and the electromagnetic field analysis method [8-9]. Data analysis method will detect physical characteristic signal, to identify the motor running state according to the characteristics of information and status, so as to realize the motor fault diagnosis. But some kind of motor fault (air gap eccentric fault) is hardly to be experimental simulated by data analysis method and characteristic value cannot be obtained quantitatively.

Method based on mathematical models [10-12] need to transform the motor equivalent circuit, and do parameter reduction establish mathematical model. But for the fault motor, electromagnetic relations are more complex than normal motor, so it is difficult to establish an accurate mathematical model of fault motor. The Ansoft software based on magnetic field analysis use the finite element discrete form to calculate, establish various motor models, which has the advantage of easy to adjust parameters, accurate and reliable design, can simulate different state of motors qualitatively and quantitatively.

This paper applied Ansoft software to establish the model of induction motor with different fault degree of different fault types, the application of the finite element analysis method is used to calculate the fault model and extract characteristics value in stator

current under different fault conditions, finally compared with the experimental data, verified the correctness of induction motor fault feature extracted based on Ansoft.

2. Theoretical Analysis

According to the principle of electric machinery[13],after induction motor with load, in order to keep the main magnetic flux within air gap basically remain unchanged, in addition to the excitation component I_m in stator current, rotor magnetomotive force will also produce a compensation "load component" I_{l1} . The stator magnetomotive force F_1 can be divided into two parts: one part is the main magnetic flux excitation magnetomotive force F_m , another part $-F_2$ is load component to offset the rotor magnetomotive force, the equation for the magnetomotive force of induction motor is as shown below:

$$F_m + F_2 = F_1 \quad (1).$$

Figure 1 shows the relationship between rotor and stator magnetomotive force and the relationship between the stator current magnetizing current and rotor current. When motor with load, fundamental wave of rotor magnetomotive force has "the rotor response" to the air gap magnetic field, the response will change the size and spatial phase of the air gap magnetic field, which will cause the stator induction electromotive force E_1 and stator current I_1 to change.

When different types of the rotor broken bar fault occurs, mechanical structure of the rotor will no longer be symmetrical, rotor magnetomotive force will change by the influence of electromagnetic induction effect, then under the influence of the rotor response, the stator current will also be changed in different extent. When the stator inter turn short circuit fault occurs, the symmetry of the electromagnetic field changes, which will induce specific frequency harmonic components in the stator current. When air gap eccentricity occurs, the main magnetic flux in air gap is changed, according to diagram 1, Stator、 rotor current phasor diagram and magnetomotive force Space vector diagram, the asymmetric caused by air gap eccentricity induce specific frequency harmonic components in the stator current.

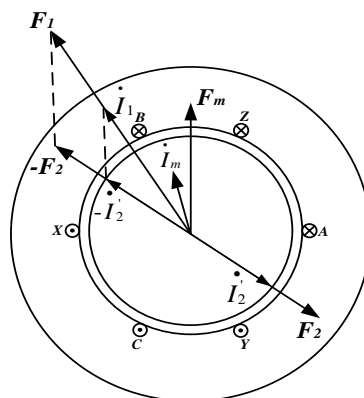


Figure 1. Stator Rotor Current Phasor and Magnetomotive Force Space Vector Diagram

3. The Finite Element Model and Fault Characteristic Quantity

In this paper, used the finite element software Ansoft to establish the induction motor model, basic parameters of the model are: rated power $P_N = 7.5kW$, rated voltage $U_N = 380v$, pole number $P=4$, the number of stator slot is 36, the number of rotor slot is 26, coil number of per winding slot is 100, length of air gap is 0.4mm.

3.1. Broken Rotor Bar

This paper separately established broken bar fault motor models of different broken bar number and different relative position with light load and full load. Model is as shown in Figure 2, Figure a is a normal motor, Figure b is one broken bar fault model. When established two broken bars model, fixed a broken bar location first, and then made another broken bar appeared respectively at a homopolar, adjacent electrode and a counter electrode of the first broken bar, to simulate failure of different asymmetries, fault location was marked in red. Similarly three broken bars model made broken bars appeared at one pole、two Poles and three poles respectively to simulate different degree asymmetry. Figure 3 and 4 are the stator current spectrum of different kind of broken bar fault model under different load conditions.

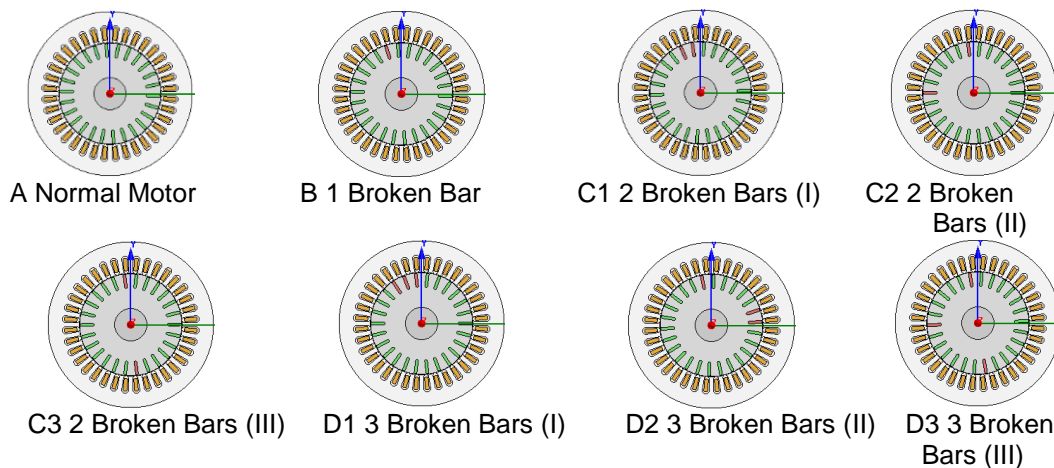


Figure 2. Broken Bar Fault Schematic Diagram

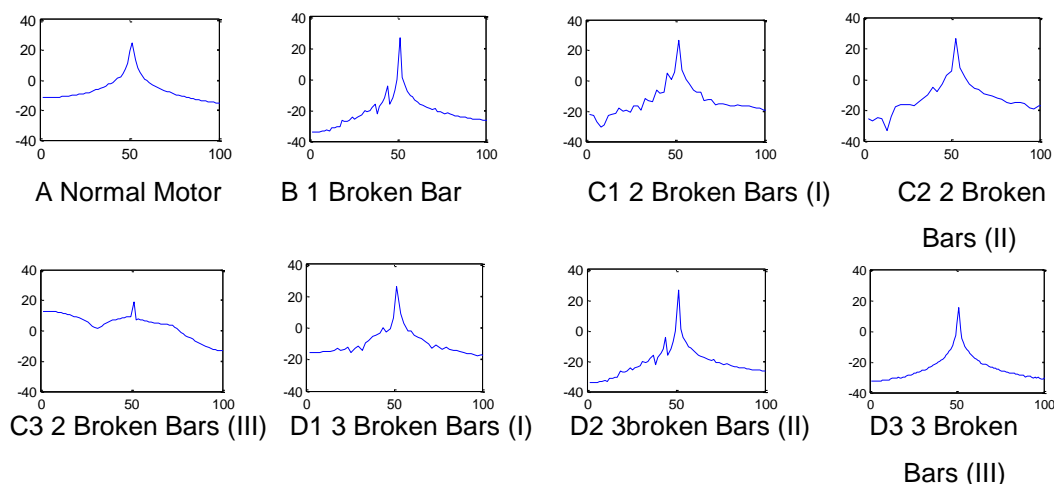


Figure 3. Stator Current Spectrum of Different Broken Bar Fault Model Under Light Load Condition

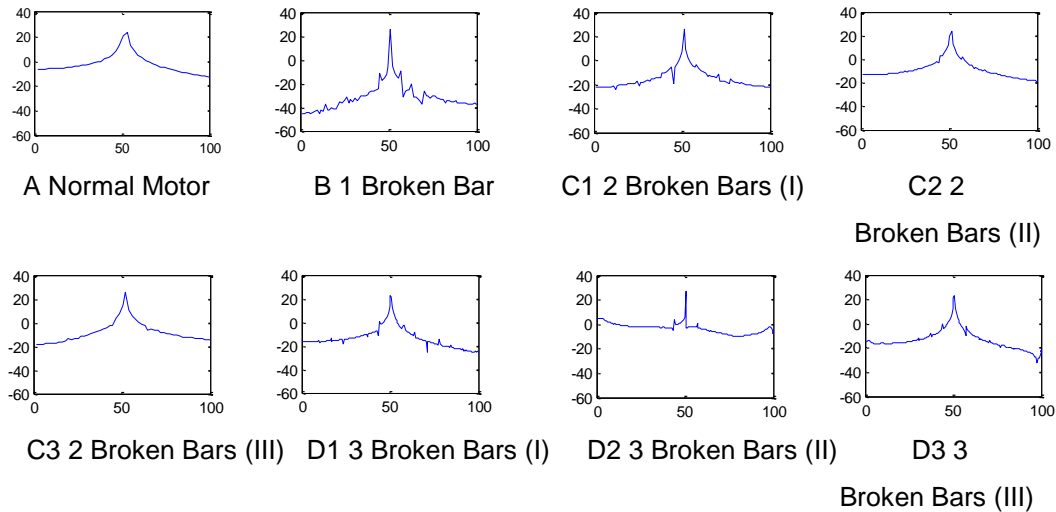


Figure 4. Stator Current Spectrum of Different Bar Fault Models Under Full Load Condition

As shown in Figure 3 and Figure 4:

1. The fault characteristics of stator current of the same fault type under different load conditions are different, the larger of the load, the more obvious of the fault characteristics.
2. The same number of broken bars but different fault location, which location caused motor greater asymmetry, the fault feature will be more obvious.
3. For the same fault condition, if broken bars in different positions, slip S will different, fault feature appears in different position of the spectrum, and its magnitude is different.

3.2. The Stator Winding Inter-Turn Short Circuit

In the finite element model of intact motor, there is 100 turn coils in each slot for each phase of the stator winding. Reduce the number of turns of the coil in each slot to simulate stator winding 15 turns, 20 turns, 25 turns, 30 turns, 50 turns, 70 turns coil winding inter-turn short circuit fault respectively. Figure 5 is the spectrum graph of stator current under different fault degree conditions, Table 1 for all harmonic contents under different inter-turn short circuit fault of stator current.

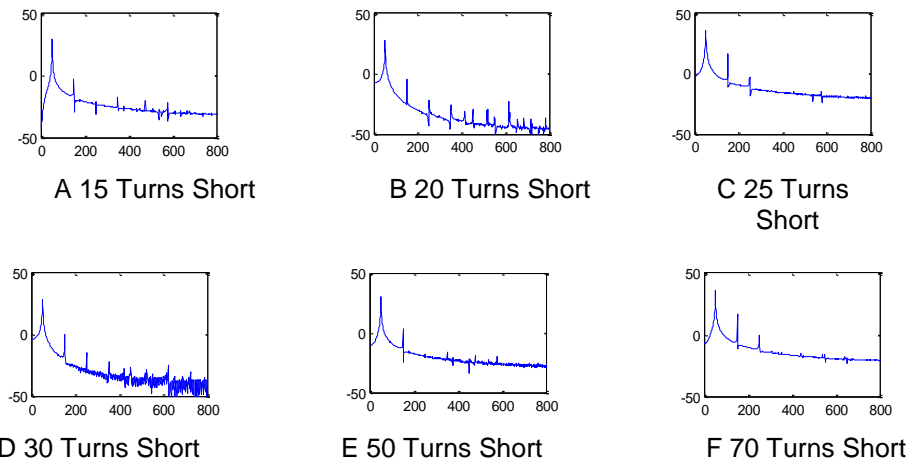


Figure 5. Stator Current Spectrum Under Different Short Circuit Condition

Table 1. The Harmonic Contents in the Stator Current under Different Short Circuit Condition

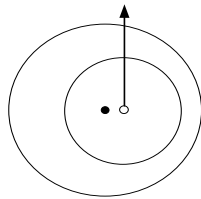
Shorted turn (turns) Harmonic content (DB)	15	20	25	30	50	70
3th	-5	-4.4	-3	3.5	16.3	16.5
5th	-22	-23	-18	-15	-2.6	-0.1
7th	-26	-19	-22	16	-14	-14.2
9th	-30	-23	-27	-21	-15	-15.1
11th	-36	-28	-48	-23	-19	-15.5
13th	-48	-35	-55	-27	-23	-23.5

Figure 5 and Table 1 shows:

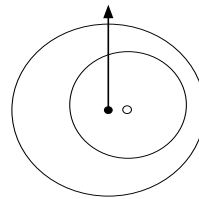
1. The harmonics in the stator current changed under different fault conditions.
2. With the deepening of short circuit, third, fifth, seventh harmonic contents increased significantly.

3.3. Air Gap Eccentricity Fault

Air gap eccentricity is divided into static eccentricity (a) and dynamic eccentricity (b). When static eccentricity fault occurs, the rotor takes its geometric center as the axis of rotation, the eccentric position fixed; when dynamic eccentricity fault occurs, the rotor takes stator's geometric center as the axis of rotation, the eccentric position changing. Air gap eccentricity diagrammatic sketch as shown in Figure 6, hollow circle point as the geometric center of the stator, solid circle point as the geometric center of the rotor, the direction of the arrow dot for rotor rotation center. In the actual electrical machinery, the two kinds of eccentric exist at the same time.



A Static Eccentricity Schematic

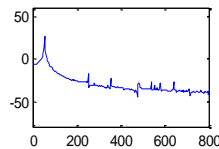


B Dynamic Eccentricity Schematic

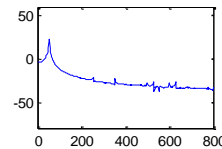
Figure 6. The Two Kinds Air Gap Eccentricity Diagrammatic Sketch

1. Static Air Gap Eccentricity

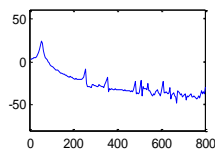
The finite element model of air gap length is 0.4mm, respectively set air gap static eccentricity of 0.1mm and 0.3mm, and experiments were conducted with light load and full load. Figure 7 for different situations of static eccentricity of stator current spectrum.



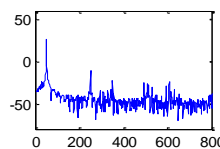
A 0.1mm Eccentricity with Light Load



B 0.1mm Eccentricity with Full Load



C 0.3mm Eccentricity with Light Load



D 0.3mm Eccentricity with Full Load

Figure7. Stator Current Spectrum of Static Air Gap Eccentricity Fault Model Under Different Load Condition

2. Dynamic Air Gap Eccentricity

The dynamic air gap eccentricity 0.1mm and 0.3mm were respectively set in the finite element models, and carried out experiments with light load and full load. Figure 8 gives dynamic eccentric stator current spectrum for different situations.

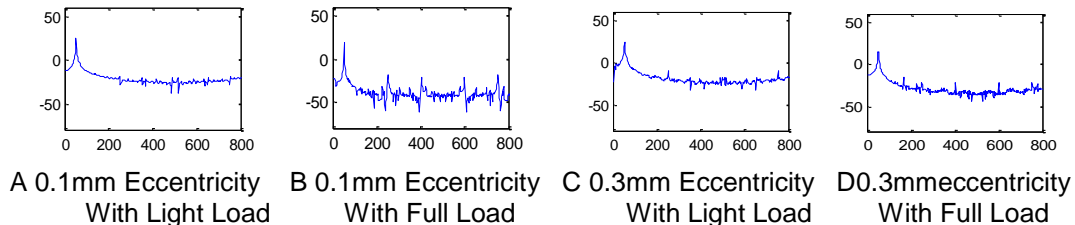


Figure 8. Stator Current Spectrum of Dynamic Air Gap Eccentricity Fault Model Under Different Load Condition

Figure 7 and Figure 8 shows:

1. when static air gap eccentricity occurs, 25Hz and 75Hz harmonics will appear in stator current ,meanwhile fifth, seventh, tenth, twelfth harmonics increase. More serious the eccentric is and much bigger the load is, more obvious the fault features are.

2. when dynamic air gap eccentricity occurs, 25Hz and 75Hz harmonics will appear in stator current ,meanwhile second、 fifth、 seventh、 eighth、 tenth、 twelfth、 thirteenth、 fifteenth harmonics increase. More serious the eccentric is, much bigger the load is, more obvious the fault features are.

4. Experiment

To verify the motor fault characteristics of Ansoft obtained by finite element analysis, established motor fault diagnosis platform, as shown in Figure 9. The experimental model of motor is YM132-4, $P_N = 7.5kW$, $U_N = 380v$, stator slot number is 36, the number of rotor slots is 26, air gap length is 0.4mm. Experiments were carried out in different fault conditions of the motor, acquired change of fault characteristics in stator current, compared with the results of finite element analysis, and then summed up the fault characteristic rules.



Figure 9. The Experimental Platform

4.1. Experiments of Broken Bars

This paper respectively carried out experiments of normal condition, 1, 2, 3 broken bars motor fault and set different relative position of bars with light load and full load.

Figure 10 and 11 are for the stator current spectrum of different fault model with light and full load.

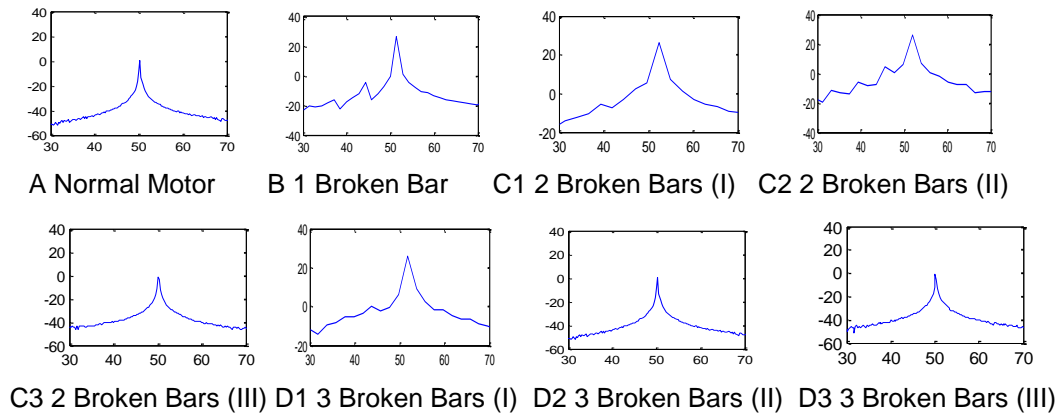


Figure 10. Stator Current Spectrum of Different Broken Bar Fault Under Light Load Condition

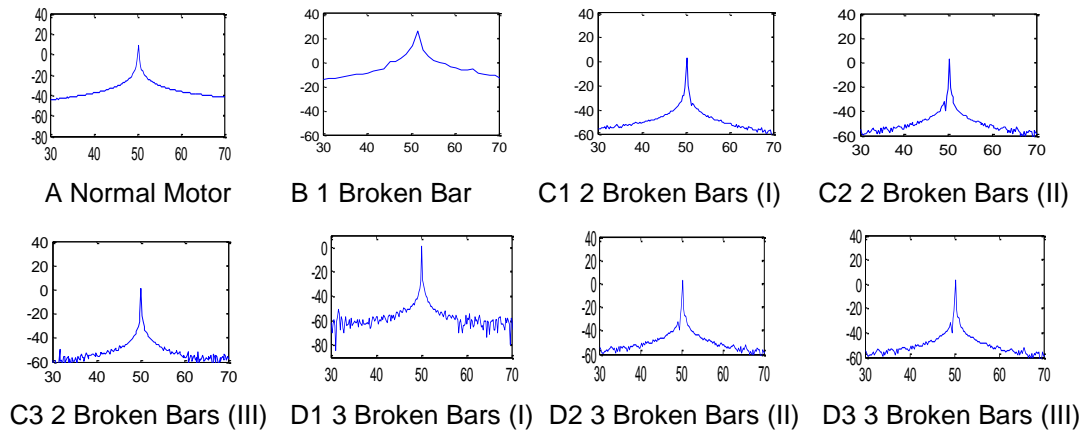


Figure 11. Stator Current Spectrum of Different Broken Bar Fault Under Full Load Condition

Figure 10 and Figure 11 shows, the quantity of broken bar fault characteristic ($1 \pm 2ks$) f not only have relationship with broken bar number but also with relative position of broken bars. Experiment results were consistent with the analysis of finite element model.

4.2. The Experiment of Stator Winding Inter Turn Short Circuit

In the experiment on the motor, winding of phase A connected with a sliding rheostat as short circuit resistance, by adjusting rheostat resistance size, to simulate the different degree of inter turn short circuit fault. Experimental schematic diagram shown in Figure 12. Figure 13 is stator current spectrum when sliding rheostat resistance values were respectively $15K\Omega$, $16.7k\Omega$, $20K\Omega$, $30K\Omega$, $100k\Omega$. Table 2 for all harmonic contents under different inter turn short circuit fault of stator current.

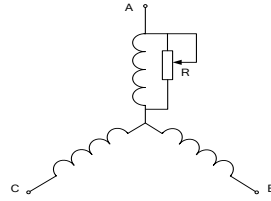


Figure 12. Inter Turn Short Circuit Schematic Diagram

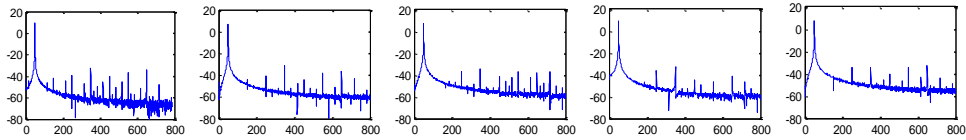


Figure 13. Stator Current Spectrum under Different Short Circuit Condition

Table2. The Measured Harmonic Contents in the Stator Current under Different Short Circuit Condition

Shorted turns (turns) Harmonic content (DB)	15	16.7	20	30	100
3th	17.8	20.6	21.9	23	24.5
5th	16.7	22.1	22.7	25.1	26.6
7th	25.1	27.5	27.4	28.8	29.2
9th	18.8	23	14.5	18.9	20.3
11th	20.9	22.8	18.6	2.1	23.9
13th	28.2	24.4	20.2	21	24.8

Results shown in Figure 12 and Table 2 were the same as the results of finite element analysis, the harmonics in the stator current change with the evolution of short circuit fault degree.

4.3. Gap Eccentric Experiment

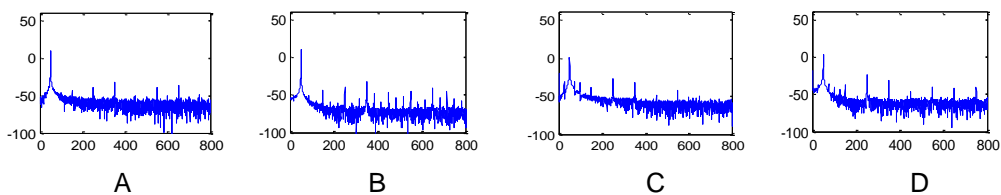


Figure 14. Stator Current Spectrum of Different Degree Air Gap Eccentricity Fault

Figure 14 for the stator current spectrum obtained under different degree of motor eccentricity fault.

We can see from Figure 14: when mixed air gap eccentricity occurs, 25Hz and 75Hz harmonics will appear in stator current, meanwhile the second, tenth, twelfth even harmonics and third, fifth, seventh, thirteenth, fifteenth odd harmonics increase obviously. Quantity of harmonic changed with eccentric degree.

5. Conclusion

In this paper, using finite element analysis software Ansoft to establish the induction motor broken bar, different degree of inter turn short circuit and air gap eccentric fault model, obtained fault characteristics of stator current, analyzed and compared through experimental method, verified the fault feature extraction method of Ansoft based on finite element analysis, and reached the following conclusions:

- 1 When broken bar fault occurs, The quantity of fault characteristic $(1 \pm 2k)f$ in stator current is not only related with the broken bar number, but also with the fault location, fault cause motor asymmetry is greater, the fault features are more obvious.
- 2 If the stator winding inter turn short circuit fault degree is different, harmonics contents in stator current is different. With the deepening of short circuit, third, fifth, seventh harmonic contents significantly increased. Other harmonic contents also increased but the growth trend is not monotone, when the fault is deepened to a certain extent, the harmonic content began to decrease, and then increase with the fault degree deepens.
- 3 when static air gap eccentricity occurs, 25Hz and 75Hz harmonics will appear in stator current, meanwhile third, fifth, seventh, tenth, twelfth harmonics increase. when dynamic air gap eccentricity occurs, 25Hz and 75Hz harmonics will appear in stator current, meanwhile, second, fifth, seventh, eighth, tenth, twelfth, thirteenth, fifteenth harmonics increase. These conclusions provide basis for judging the fault type, fault degree and development trend.

References

- [1] Y. Shao, "Feature extracting method of stator and rotor faults of induction motor by park vector rotating filter [J]", *ELECTRIC MACHINES AND CONTROL*, 2010, 14(3)57-61.
- [2] Y.H. Hu, Z.L. Zhang, F. Li and M/R. Zhang, "Diagnosis analysis of rotor system based on holospectrum[J]", *JOURNAL OF VIBRATION AND SHOCK*, 2009, 28(12) 164-166
- [3] T.B. Sun, J. Chen and G. Zhang, "Study on holospectrum based on correction of phase difference [J]" *JOURNAL OF VIBRATION AND SHOCK*, 2009, 28(8) 99-102
- [4] X/H. Wang , "Method of Fault Diagnosis for Induction Machine Rotor Broken Bar Based on Wavelet Package and Elman Neural Network [J]" *Journal of Hunan University (Natural Sciences)*, 2010 37(5) 45-48.
- [5] F/L. Niu and J. Huang, "Rotor Fault Detection for Induction Motors Based Complex Analytical Wavelet Transform of Electromagnetic Torque [J]" *TRANSACTIONS OF CHINA ELECTROTECHNICAL SOCIETY*, 2005, 20(7) 100-105. .
- [6] L. Han and L/P. Shi, "Study of the Induction Motor Faulted Diagnosis Based on Information Fusion Technology[J]" , *Journal of China University of Mining & Technology*, 2010, 39(2)178-184. .
- [7] L. Han and L/P. Shi, "Fault diagnosis of induction motor based on information entropy fusion [J]", *ICACC 2010*, 48-51.
- [8] X. Ying and L/C. Wang, "Magnetic Field Variation in Squirrel-cage Induction Motor Operating on Asymmetric Rotor [J]", *Proceedings of the CSEE*, 2011, 31(30) 100-108.
- [9] X. Ying, "Performance evaluation and thermal fields analysis of induction motor with broken rotor bars located at different relative positions [J]", *IEEE Trans. On Magnetics*, 2010, 46(5) 1243-1250.
- [10] X/D. Li and Q. Wu, "Nandi S. Performance analysis of a three-phase induction machine with inclined static eccentricity[J]", *IEEE Transactions on Industry Annlications* , 2007. 43(21): 531-541.
- [11] Y/L. He, S/T. Sun, G/J. Tang and L. Xiang, "Eccentric fault level identification of a turbo generator based on stator vibration characteristics[J]", *JOURNAL OF VIBRATION AND SHOCK*, 2012, 31(22) 53-57.
- [12] J/J Li, J/B. Sheng, G. Wang and H. Wei, "Research on Parameter Identification Method for Induction Motor [J]", *TRANSACTIONS OF CHINA ELECTROTECHNICAL SOCIETY* 2006, 21(1) 70-74.
- [13] Y/Q. Tang, "ShiNai .Electric machinery [M]", BeijingChina Machine Press , 2005, 163-192.
- [14] X/H. Bao and Q. Lu, "Review and Prospect of Air-gap Eccentricity Faults in Induction Machines [J]", *Proceedings of the CSEE*, 2013, 33 (6): 93-98.
- [15] P.P. Wang, L/P. Shi and C/X. Miao, "HanLi. Diagnosing Stator Fault in Motor by Using Bare-bone Particle Swarm Optimization algorithm and SVM [J]", *ELECTRIC MACHINES AND CONTROL* 2013, 17(2):48-54

- [16] L. U. Werner, "Theoretical analysis of shaft vibrations in two-pole induction machines considering static rotor eccentricity [C]", International Symposium on Power Electronics Electrical Drives Automation and Motion, Pisa Italy: IEEE2010: 853-860.
- [17] J. Sprooten and J.C. Maun, "Influence of saturation level on the effect of broken bars in induction motors using fundamental electromagnetic laws and finite element simulations[J]", IEEE Trans. on Energy Conversion 2009, 24(3): 557-564.

Authors



Xiaolei Zhang, She is currently a master student at School of Information and Electrical Engineering in *China University of Mining and Technology*. Her research interests are electrical equipment fault diagnosis, industrial automation systems and intelligent control of wind turbines.



Han Li, She was born in 1977. She received her master's degree at North China Electric Power University, Southeast University Ph.D. She is a professor at School of Information and Electrical Engineering in *China University of Mining and Technology*. Her research interests are electrical equipment fault diagnosis, artificial intelligence research, and micro-grid technology.